SUPPORTING INFORMATION

Synthesis, Characterization, and Thermal Properties of Volatile 1,4-Dialkyl-5-silatetrazolines: Nitrogen-Rich Silicon Heterocycles as Possible CVD Precursors to Silicon Nitride

*Vincent J. Flores and Gregory S. Girolami**

School of Chemical Sciences, University of Illinois at Urbana-Champaign,

600 S. Mathews Ave., Urbana, IL 61801

Email address: ggirolam@illinois.edu

TABLE OF CONTENTS

Crystal Structure Analyses S2

Thermogravimetric Analysis Plots S9

NMR Spectra S15

IR Spectra..... S24

Crystal Structure Analyses.

[1,4-Di(*tert*-butyl)-1,4-diazabut-2-ene-1,4-diyl](1,4-diethyltetraaz-2-ene-1,4-diyl)-silane, 6,9-Di-*tert*-butyl-1,4-diethyl-1,2,3,4,6,9-hexaaza-5-silaspiro[4.4]nona-2,7-diene, 2. Single crystals of the ethyl-substituted compound **2** were mounted on glass fibers with Krytox oil (DuPont) and immediately cooled to -75 °C in a cold nitrogen gas stream on the diffractometer. Standard peak search and indexing procedures gave rough cell dimensions, and least squares refinement using 20876 reflections yielded the cell dimensions given in Table 1.

Data were collected with a Bruker Apex-II CCD diffractometer by using the measurement parameters listed in Table 1. The orthorhombic lattice and the average values of the normalized structure factors suggested the space group $Pna2_1$, which was confirmed by the success of the subsequent refinement. The measured intensities were reduced to structure factor amplitudes and their esd's by correction for background, scan speed, and Lorentz and polarization effects. No corrections for crystal decay or absorption were necessary. Systematically absent reflections were deleted and symmetry equivalent reflections were averaged to yield the set of unique data. One reflection (1 1 0) was found to be a statistical outlier remaining 5541 unique data were used in the least squares refinement.

The structure was solved using direct methods (SHELXS). Correct positions for all the non-hydrogen atoms were deduced from an E-map. Subsequent least-squares refinement and difference Fourier calculations revealed the positions of the hydrogen atoms. The quantity minimized by the least-squares program was $\Sigma w(F_o^2 - F_c^2)^2$, where $w = \{[\sigma(F_o^2)]^2 + (0.0463P)^2 + 0.30P\}^{-1}$ and $P = (F_o^2 + 2F_c^2)/3$. The analytical approximations to the scattering factors were used, and all structure factors were corrected for both real and imaginary components of anomalous dispersion. In the final cycle of least squares, independent anisotropic displacement factors were refined for the non-hydrogen atoms. Hydrogen atoms were placed in idealized positions; the

methyl groups were allowed to rotate about the C-C axis to find the best least-squares positions. The displacement parameters for methylene hydrogens were set equal to 1.2 times U_{eq} for the attached carbon; those for methyl hydrogens were set to 1.5 times U_{eq}. No correction for isotropic extinction was necessary. Successful convergence was indicated by the maximum shift/error of 0.001 for the last cycle. Final refinement parameters are given in Table 1. The largest peak in the final Fourier difference map (0.33 eÅ^{-3}) was located 0.75 Å from C7. A final analysis of variance between observed and calculated structure factors showed no apparent errors.

[1,4-Di(*tert*-butyl)-1,4-diazabut-2-ene-1,4-diyl][1,4-di(*iso*-propyl)tetraaz-2-ene-1,4-diyl]silane, 6,9-Di-*tert*-butyl-1,4-di(*iso*-propyl)-1,2,3,4,6,9-hexaaza-5-silaspiro[4.4]nona-2,7-diene, 3. Single crystals of the *iso*-propyl substituted compound **3** were mounted on glass fibers with Krytox oil (DuPont) and immediately cooled to -75 °C in a cold nitrogen gas stream on the diffractometer. Standard peak search and indexing procedures gave rough cell dimensions, and least squares refinement using 12553 reflections yielded the cell dimensions given in Table 1.

Data were collected with a Bruker Apex-II CCD diffractometer by using the measurement parameters listed in Table 1. The triclinic lattice and the average values of the normalized structure factors suggested the space group P1, which was confirmed by the success of the subsequent refinement. The measured intensities were reduced to structure factor amplitudes and their esd's by correction for background, scan speed, and Lorentz and polarization effects. No corrections for crystal decay but a multi-scan absorption correction was applied, the minimum and maximum transmission factors being 0.7079 and 0.7454. Systematically absent reflections were deleted and symmetry equivalent reflections were averaged to yield the set of unique data. Three reflections (0 -1 2, 5 -8 5, and 0 1 0) were found to be a statistical outliers; the remaining 8049 unique data were used in the least squares refinement.

The structure was solved using direct methods (SHELXS). Correct positions for all the

non-hydrogen atoms were deduced from an E-map. Subsequent least-squares refinement and difference Fourier calculations revealed the positions of the hydrogen atoms. The quantity minimized by the least-squares program was $\Sigma w(F_o^2 - F_c^2)^2$, where $w = \{[\sigma(F_o^2)]^2 + (0.0393P)^2 + 0.27P\}^{-1}$ and $P = (F_o^2 + 2F_c^2)/3$. The analytical approximations to the scattering factors were used, and all structure factors were corrected for both real and imaginary components of anomalous dispersion. In the final cycle of least squares, independent anisotropic displacement factors were refined for the non-hydrogen atoms. Hydrogen atoms were placed in idealized positions; the methyl groups were allowed to rotate about the C-C axis to find the best least-squares positions. The displacement parameters for methine hydrogens were set equal to 1.2 times U_{eq} for the attached carbon; those for methyl hydrogens were set to 1.5 times U_{eq}. No correction for isotropic extinction was necessary. Analysis of the diffraction intensities suggested the presence of inversion twinning; therefore, the intensities were calculated from the equation $I = xI_a + (1-x)I_b$, where x is a scale factor that relates the volumes of the inversion-related twin components. The scale factor refined to a value of 0.48(12). Successful convergence was indicated by the maximum shift/error of 0.000 for the last cycle. Final refinement parameters are given in Table 1. The largest peak in the final Fourier difference map (0.28 eÅ^{-3}) was located 0.78 Å from N7. A final analysis of variance between observed and calculated structure factors showed no apparent errors.

[1,4-Di(*tert*-butyl)-1,4-diazabut-2-ene-1,4-diyl][1,4-di(*tert*-butyl)tetraaz-2-ene-1,4-diyl]silane, 6,9-Di-*tert*-butyl-1,4-di(*tert*-butyl)-1,2,3,4,6,9-hexaaza-5-silaspiro[4.4]nona-2,7-diene, 4. Single crystals of the *tert*-butyl substituted compound **4** were mounted on glass fibers with Krytox oil (DuPont) and immediately cooled to -75 °C in a cold nitrogen gas stream on the diffractometer. Standard peak search and indexing procedures gave rough cell dimensions, and least squares refinement using 7478 reflections yielded the cell dimensions given in Table 1.

Data were collected with a Bruker Apex-II CCD diffractometer by using the measurement

parameters listed in Table 1. The orthorhombic lattice and the average values of the normalized structure factors suggested the space group Cmcm, which was confirmed by the success of the subsequent refinement, and this choice was confirmed by successful refinement of the proposed model. The measured intensities were reduced to structure factor amplitudes and their esd's by correction for background, scan speed, and Lorentz and polarization effects. No corrections for crystal decay were necessary, but a multi-scan absorption correction was applied, the minimum and maximum transmission factors being 0.683 and 0.746. All 1459 unique data were used in the least squares refinement.

The structure was solved using direct methods (SHELXS). Correct positions for all the non-hydrogen atoms were deduced from an E-map. Hydrogen atoms bound to C3 are disordered due to the mirror symmetry of the molecule. Subsequent least-squares refinement and difference Fourier calculations revealed the positions of the hydrogen atoms. The quantity minimized by the least-squares program was $\Sigma w(F_o^2 - F_c^2)^2$, where $w = \{[\sigma(F_o^2)]^2 + (0.0433P)^2 + 1.68P\}^{-1}$ and $P = (F_o^2 + 2F_c^2)/3$. The analytical approximations to the scattering factors were used, and all structure factors were corrected for both real and imaginary components of anomalous dispersion. In the final cycle of least squares, independent anisotropic displacement factors were refined for the non-hydrogen atoms. Hydrogen atoms were placed in idealized positions; the methyl groups were allowed to rotate about the C-C axis to find the best least-squares positions. The displacement parameters for methylene hydrogens were set equal to 1.2 times U_{eq} for the attached carbon; those for methyl hydrogens were set to 1.5 times U_{eq}. Successful convergence was indicated by the maximum shift/error of 0.000 for the last cycle. Final refinement parameters are given in Table 1. The largest peak in the final Fourier difference map (0.37 eÅ^{-3}) was located 0.67 Å from C1. A final analysis of variance between observed and calculated structure factors showed no apparent errors.

Table S1. Crystallographic Data for the 1,4-Dialkyl-5-silatetrazoline Compounds **2**−**4**.

	2	**3**	**4**
formula	$C_{14}H_{30}N_6Si$	$C_{16}H_{34}N_6Si$	$C_{18}H_{38}N_6Si$
formula weight	310.53	338.58	366.63
temp (K)	100.0	100.0	100.0
λ (deg)	0.71073	0.71073	0.71073
crystal structure	orthorhombic	triclinic	orthorhombic
space group	*Pna*2$_1$	*P*1	*Cmcm*
a (Å)	11.2805(4)	8.9917(4)	13.8746(7)
b (Å)	18.1249(7)	10.0564(4)	11.8697(7)
c (Å)	8.8655(3)	11.0337(4)	13.0995(7)
α (deg)	90	93.0697(15)	90
β (deg)	90	97.2334(17)	90
γ (deg)	90	90.9204(16)	90
V (Å^3)	1812.62(11)	988.09(7)	2157.3(2)
Z	4	2	4
ρ_{calc} (g cm^{-3})	1.138	1.138	1.129
μ (mm^{-1})	0.134	0.128	1.122
F(000)	680.0	372.0	808.0
crystal size (mm)	0.269 × 0.255 × 0.154	0.154 × 0.083 × 0.035	0.78 × 0.624 × 0.214
θ range (deg)	4.494−61.094	4.568−52.87	4.516−56.664
R(int)	0.0333	0.0356	0.0360
Abs corr type	none	multiscan	multiscan
max, min transm. factors	0.965, 0.980	0.7079, 0.7454	0.683, 0.746
data/restraints/ parameters	5541/1/198	8049/3/435	1459/0/75
goodness of fit on F^2	1.062	1.034	1.047
R_1 [$F_0 > 4\sigma(F_0)$][a]	0.0303	0.0341	0.0327
wR_2 (all data)[b]	0.0792	0.0833	0.0874
max, min $\Delta\rho_{elect}$ (e Å^{-3})	0.27, −0.21	0.28, −0.23	0.37, −0.26
flack parameter	0.00(3)	0.42(5)	none

[a] $R_1=\sum||F_o| - |F_c||/\sum|F_o|$ for reflections, where $F_o^2 > 2\sigma(F_o^2)$. [b] $wR_2= [\sum w(F_o^2-F_c^2)^2/\sum(F_o^2)^2]^{1/2}$ for all reflections.

Table S2. Selected Bond Distances and Angles for the 1,4-Diethyl-5-silatetrazoline Compound **2**.

Distances (Å)			
Si(1)-N(1)	1.7244(14)	N(3)−N(4)	1.3803(18)
Si(1)-N(2)	1.7256(13)	N(4)−N(5)	1.270(2)
Si(1)-N(3)	1.7280(13)	N(5)−N(6)	1.3805(19)
Si(1)-N(6)	1.7305(15)	N(3)−C(11)	1.460(2)
		N(6)−C(13)	1.460(2)
Angles (deg)			
Si(1)−N(3)−N(4)	114.27(10)	N(1)−Si(1)−N(2)	92.56(6)
Si(1)−N(3)−C(11)	131.60(11)	N(1)−Si(1)−N(3)	112.29(7)
Si(1)−N(6)−N(5)	114.03(11)	N(1)−Si(1)−N(6)	119.07(6)
Si(1)−N(6)−C(13)	132.67(12)	N(2)−Si(1)−N(3)	118.26(6)
N(3)−N(4)−N(5)	112.90(13)	N(2)−Si(1)−N(6)	122.31(7)
N(4)−N(5)−N(6)	113.15(13)	N(3)−Si(1)−N(6)	85.62(7)
N(4)−N(3)−C(11)	114.11(12)		
N(5)−N(6)−C(13)	113.31(14)		

Table S3. Selected Bond Distances and Angles for the 1,4-(Di-*iso*-propyl)-5-silatetrazoline Compound **3**.

Distances (Å)			
Si(1)−N(1)	1.717(2)	Si(2)−N(7)	1.711(3)
Si(1)−N(2)	1.723(3)	Si(2)−N(8)	1.721(3)
Si(1)−N(3)	1.734(2)	Si(2)−N(9)	1.729(3)
Si(1)−N(6)	1.730(3)	Si(2)−N(12)	1.735(3)
N(3)−N(4)	1.382(3)	N(9)−N(10)	1.378(3)
N(4)−N(5)	1.270(4)	N(10)−N(11)	1.277(4)
N(5)−N(6)	1.385(3)	N(11)−N(12)	1.374(4)
N(6)−C(14)	1.467(4)	N(12)−C(30)	1.472(4)
Angles (deg)			
Si(1)−N(3)−C(11)	131.2(2)	Si(2)−N(9)−C(27)	130.8(2)
Si(1)−N(3)−N(4)	113.71(19)	Si(2)−N(9)−N(10)	114.1(2)
Si(1)−N(6)−C(14)	131.4(2)	Si(2)−N(12)−C(30)	131.7(2)
Si(1)−N(6)−N(5)	113.66(19)	Si(2)−N(12)−N(11)	113.7(2)
N(1)−Si(1)−N(2)	92.96(12)	N(7)−Si(2)−N(8)	93.18(12)
N(1)−Si(1)−N(3)	119.05(12)	N(7)−Si(2)−N(9)	119.48(12)
N(1)−Si(1)−N(6)	121.74(12)	N(7)−Si(2)−N(12)	120.85(12)
N(2)−Si(1)−N(3)	119.67(13)	N(8)−Si(2)−N(9)	120.80(13)
N(2)−Si(1)−N(6)	120.42(12)	N(8)−Si(2)−N(12)	119.78(13)
N(6)−Si(1)−N(3)	86.04(12)	N(9)−Si(2)−N(12)	85.80(12)
N(4)−N(3)−C(11)	114.5(2)	N(10)−N(9)−C(27)	115.0(2)
N(3)−N(4)−N(5)	113,2(2)	N(9)−N(10)−N(9)	112.8(2)
N(4)−N(5)−N(6)	113.3(2)	N(10)−N(11)−N(12)	113.4(2)
N(5)−N(6)−C(14)	114.9(2)	N(11)−N(12)−C(30)	114.2(2)

Table S4. Selected Bond Distances and Angles for the 1,4-(Di-*tert*-butyl)-5-silatetrazoline Compound **(4)**

Distance (Å)			
Si(1)−N(1)	1.7260(11)	C(1)−C(1)[1]	1.343(3)
Si(1)−N(2)	1.7350(11)	N(2)−C(5)	1.4858(16)
N(1)−C(1)	1.4142(16)	N(2)−N(3)	1.3878(15)
N(1)−C(2)	1.4856(16)	N(3)−N(3)[2]	1.274(2)

[1] +*x*,+*y*,1/2−*z*; [2] 1−*x*,+*y*,+*z*

Angles (deg)			
Si(1)−N(1)−C(1)	109.52(8)	N(1)−Si(1)−N(1)[1]	92.72(8)
Si(1)−N(1)−C(2)	131.42(9)	N(1)−Si(1)−N(2)	120.12(3)
Si(1)−N(2)−C(5)	133.78(9)	N(2)−Si(1)−N(2)[2]	86.71(7)
Si(1)−N(2)−N(3)	113.12(8)	N(3)−N(2)−C(5)	113.10(10)
		N(2)−N(3)− N(3)[2]	113.52(7)

[1]+*x*,+*y*,1/2−*z*; [2]1−*x*,+*y*,+*z*

Thermogravimetric Analysis Plots

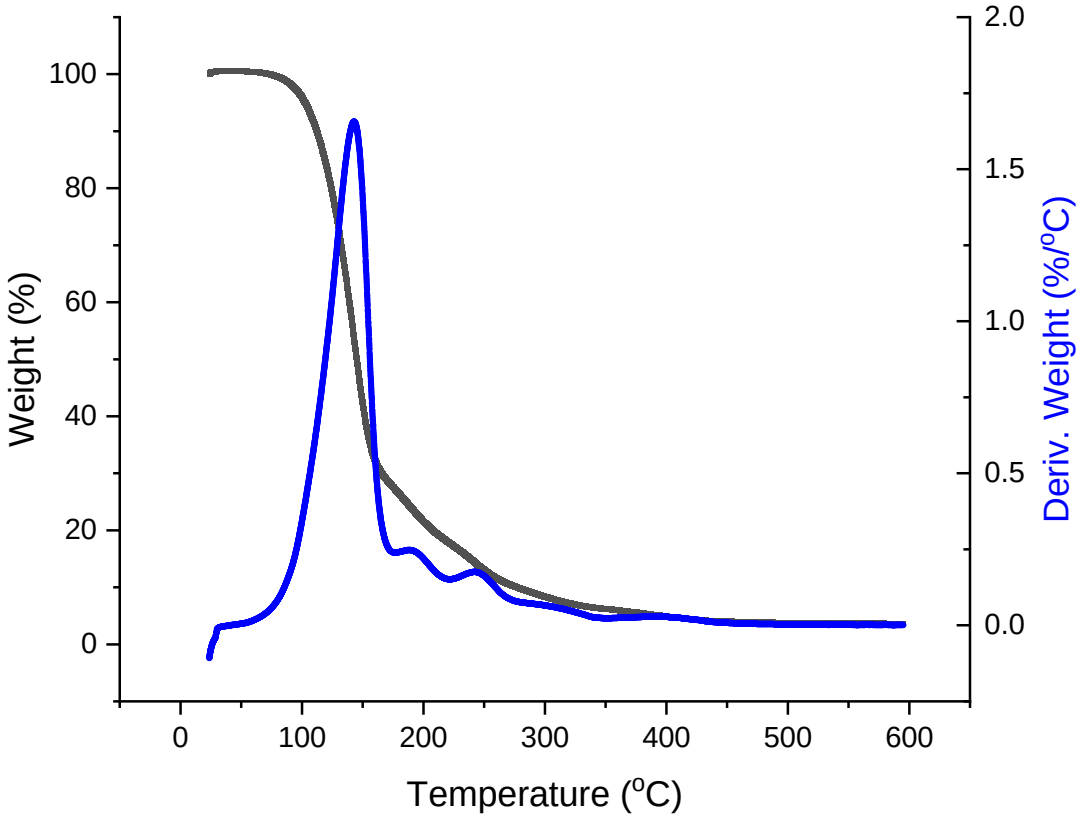

Figure S1. TGA plot of weight loss vs. temperature and derivative weight % vs. temperature for the silylene **1** under 1 atm of nitrogen at a ramp rate of 10 ºC/min.

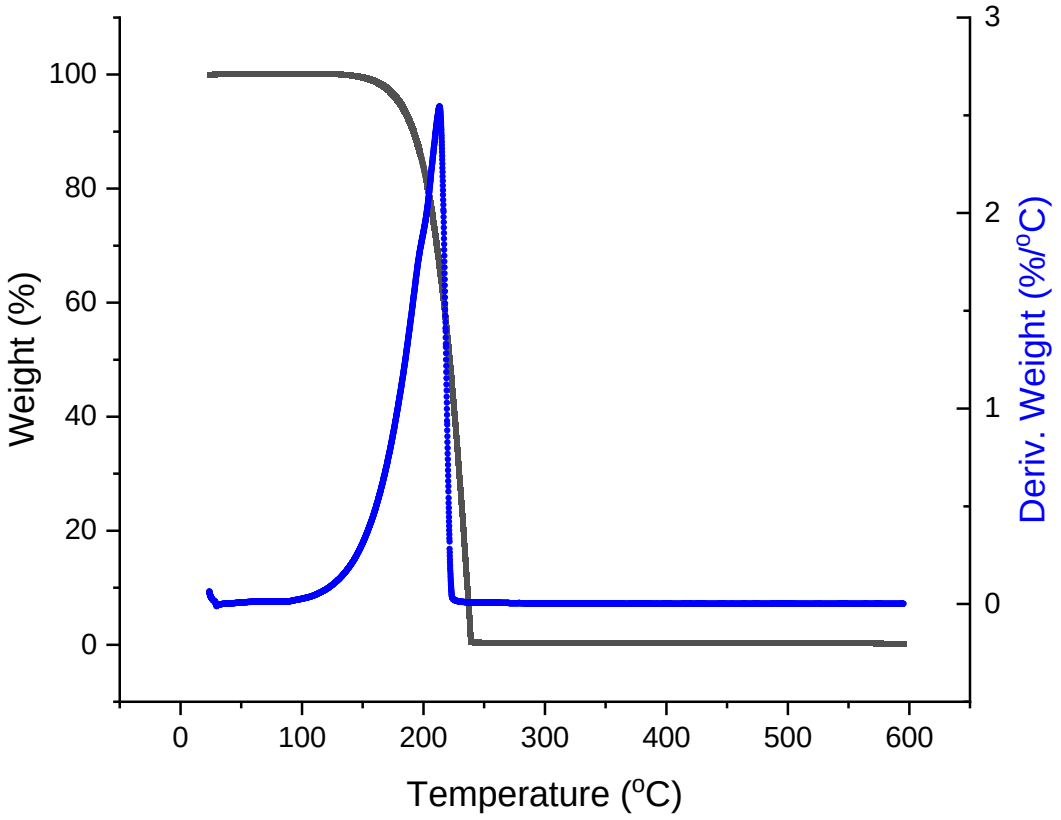

Figure S2. TGA plot of weight loss vs. temperature and derivative weight % vs. temperature for the ethyl-substituted compound **2** under 1 atm of nitrogen at a ramp rate of 10 ºC/min.

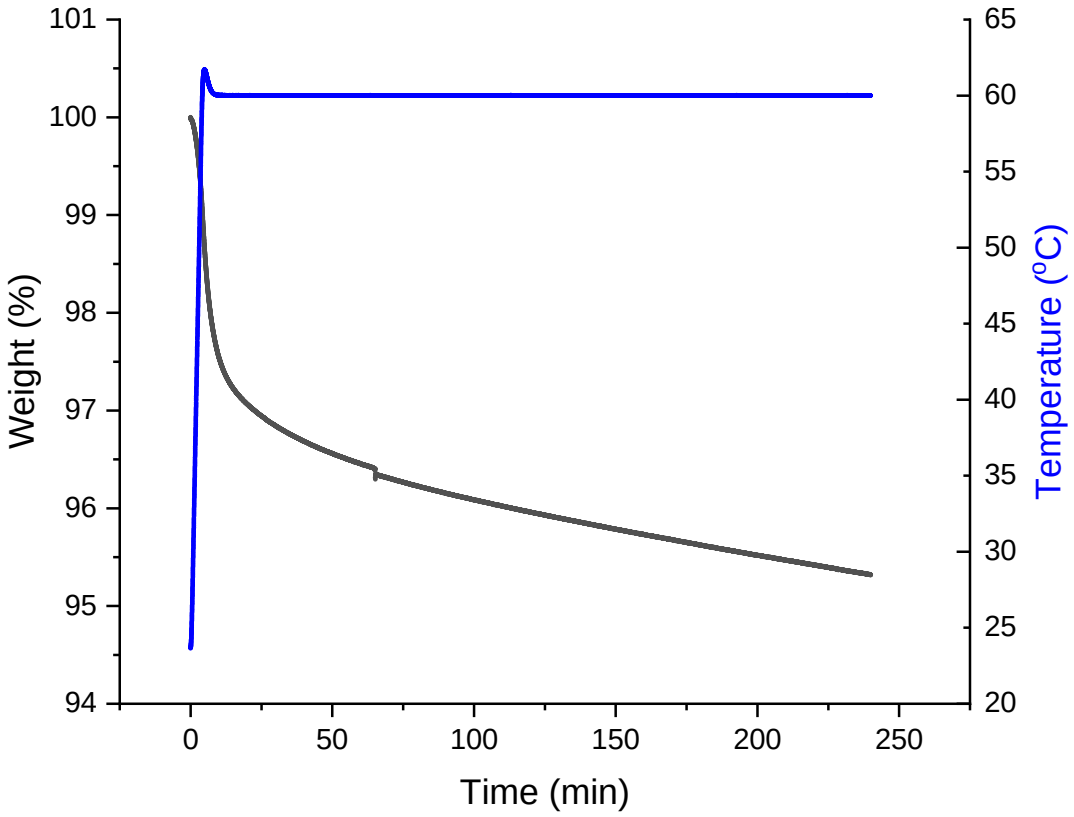

Figure S3. Isothermal TGA plot of weight % loss vs. time and temperature ºC vs. time for the ethyl-substituted compound **2** under 1 atm of nitrogen at 60 ºC for 4 hours.

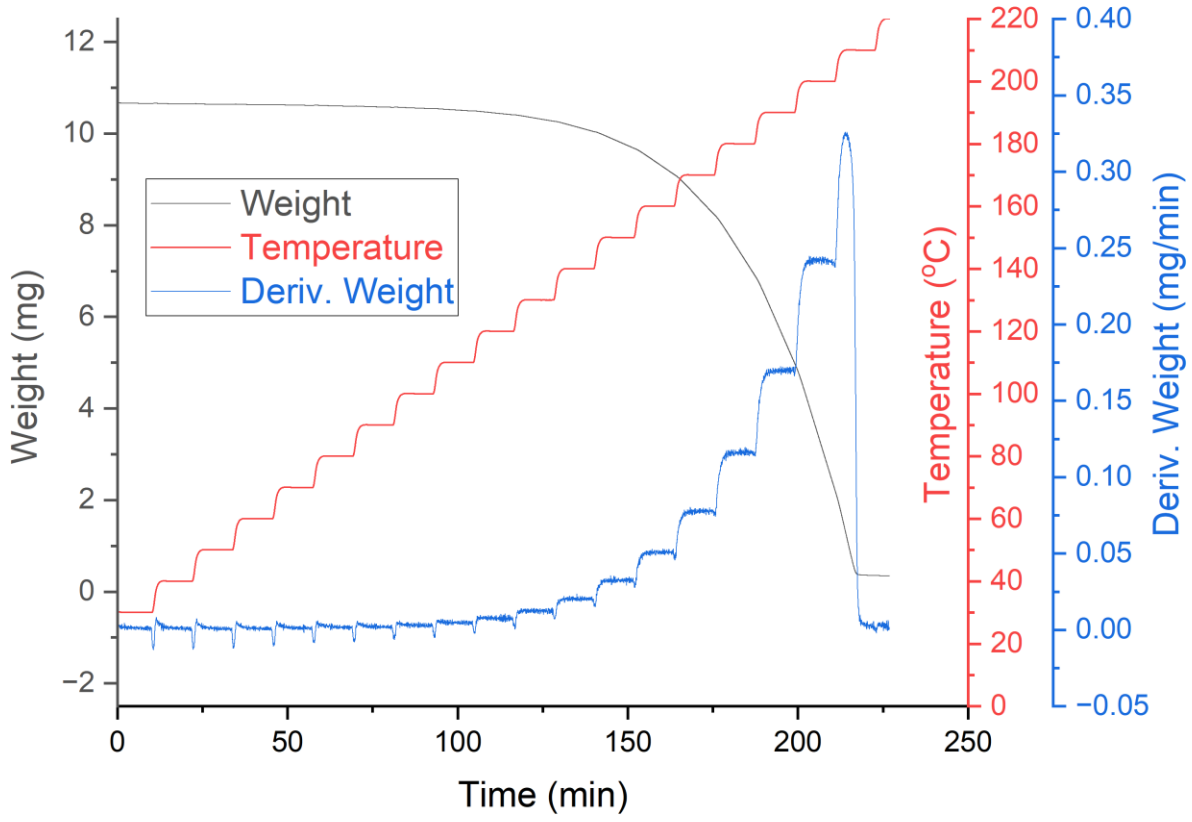

Figure S4. Stepwise isothermal TGA plot of weight loss (mg), temperature (ºC), and derivative weight % vs. time for the ethyl-substituted compound **2** under 1 atm of nitrogen with dwell times of 10 minutes in 10 ºC steps, with a ramp rate between steps of 10 ºC/min.

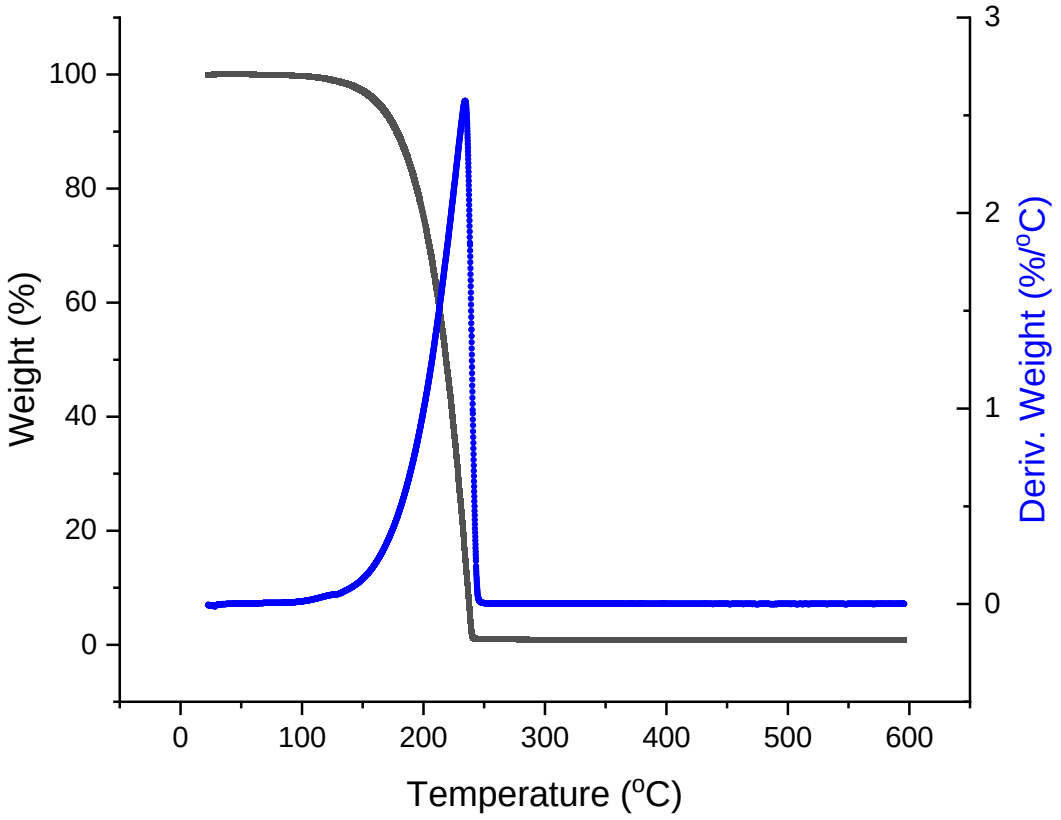

Figure S5. TGA plot of weight loss vs. temperature and derivative weight % vs. temperature for the *iso*-propyl substituted compound **3** under 1 atm of nitrogen at a ramp rate of 10 ºC/min.

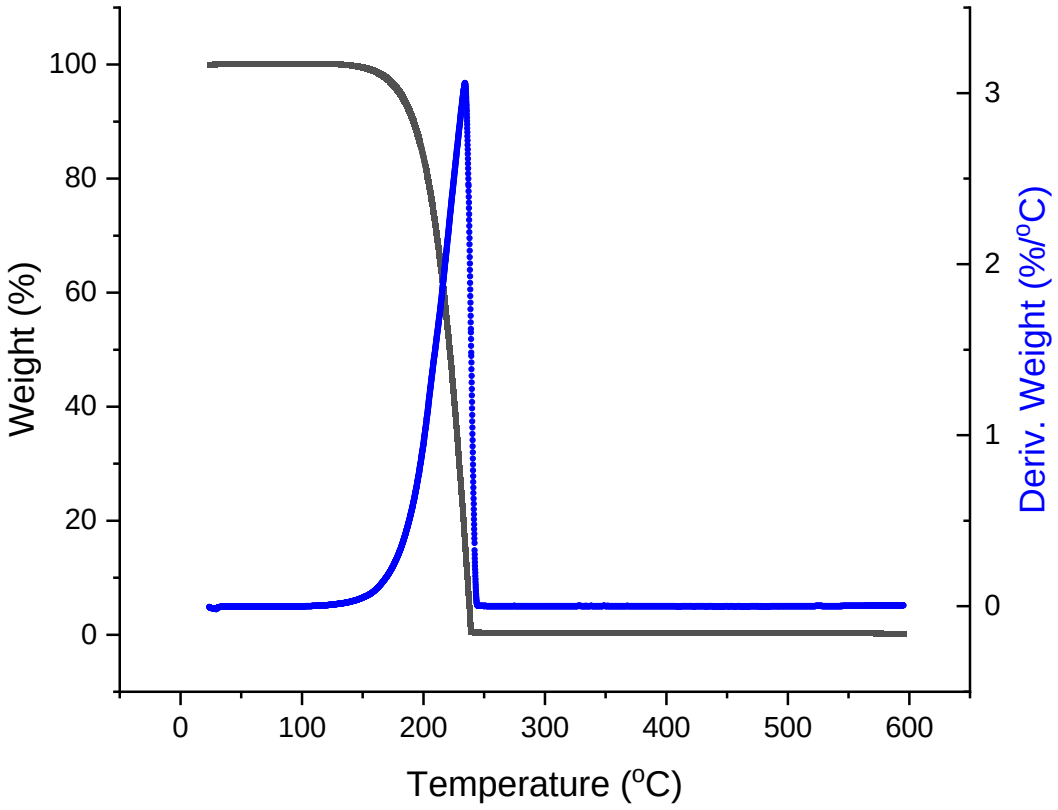

Figure S6. TGA plot of weight loss vs. temperature and derivative weight % vs. temperature for the *tert*-butyl substituted compound **4** under 1 atm of nitrogen at a ramp rate of 10 ºC/min.

NMR Spectra

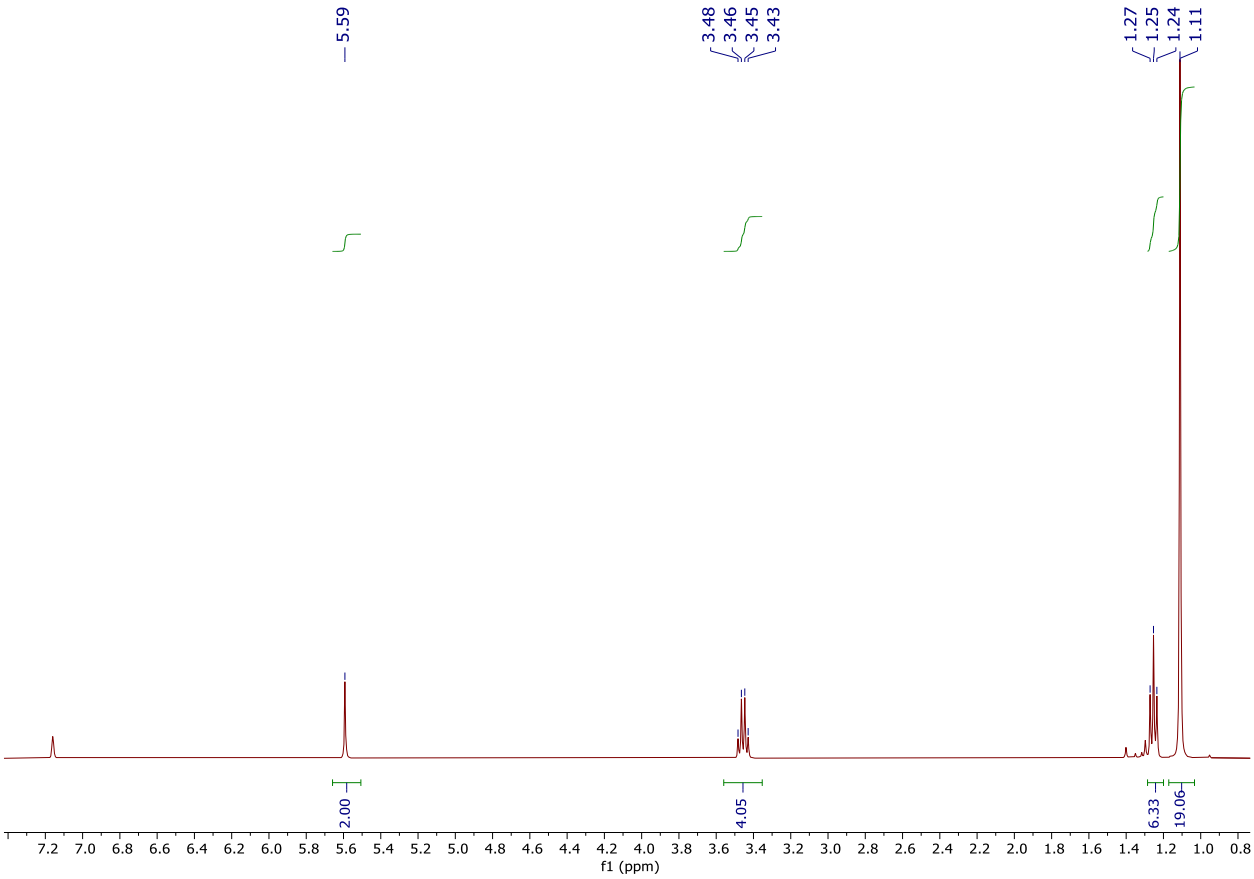

Figure S7. ^{1}H NMR spectrum of the ethyl-substituted compound **2** at 25 ºC in benzene-d_6.

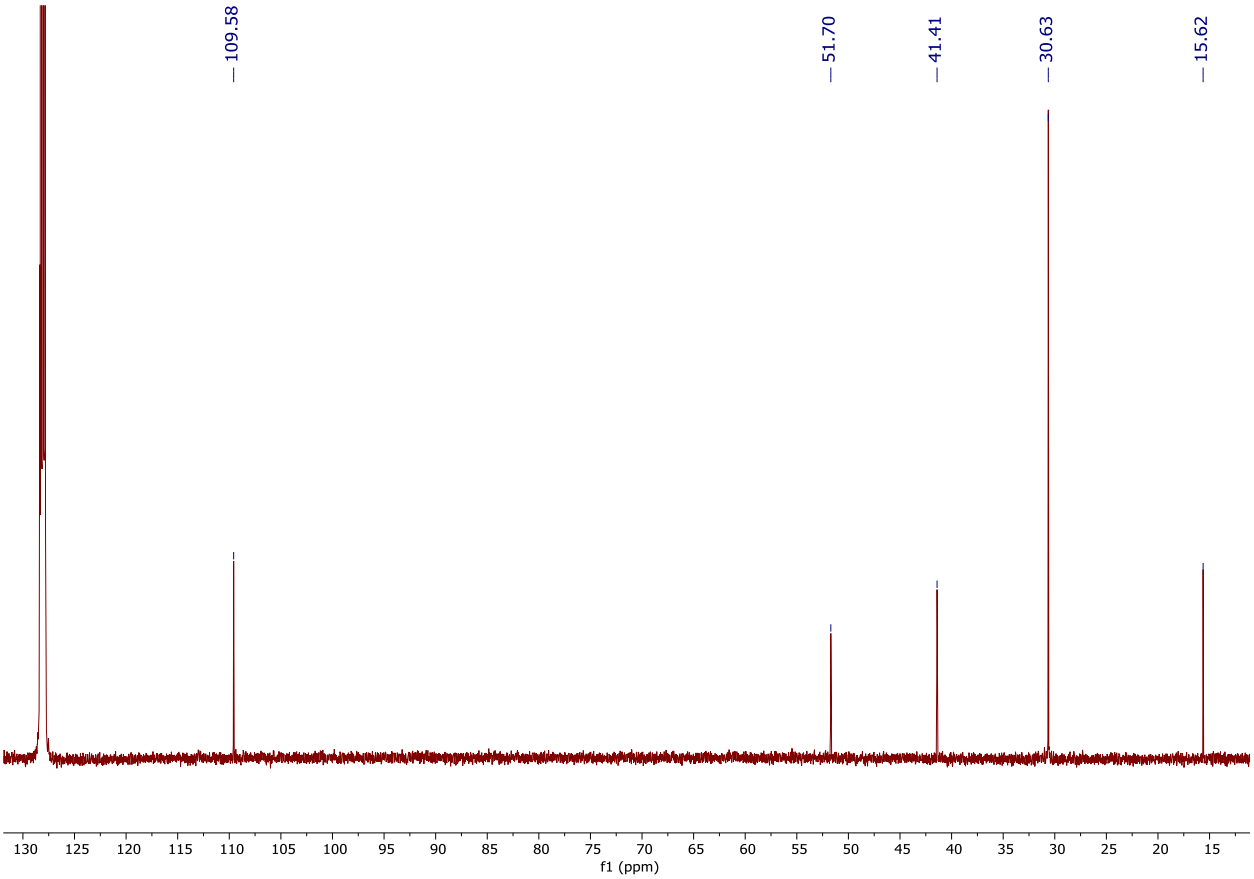

Figure S8. $^{13}C\{^{1}H\}$ NMR spectrum of the ethyl-substituted compound **2** at 25 ºC in benzene-d_6.

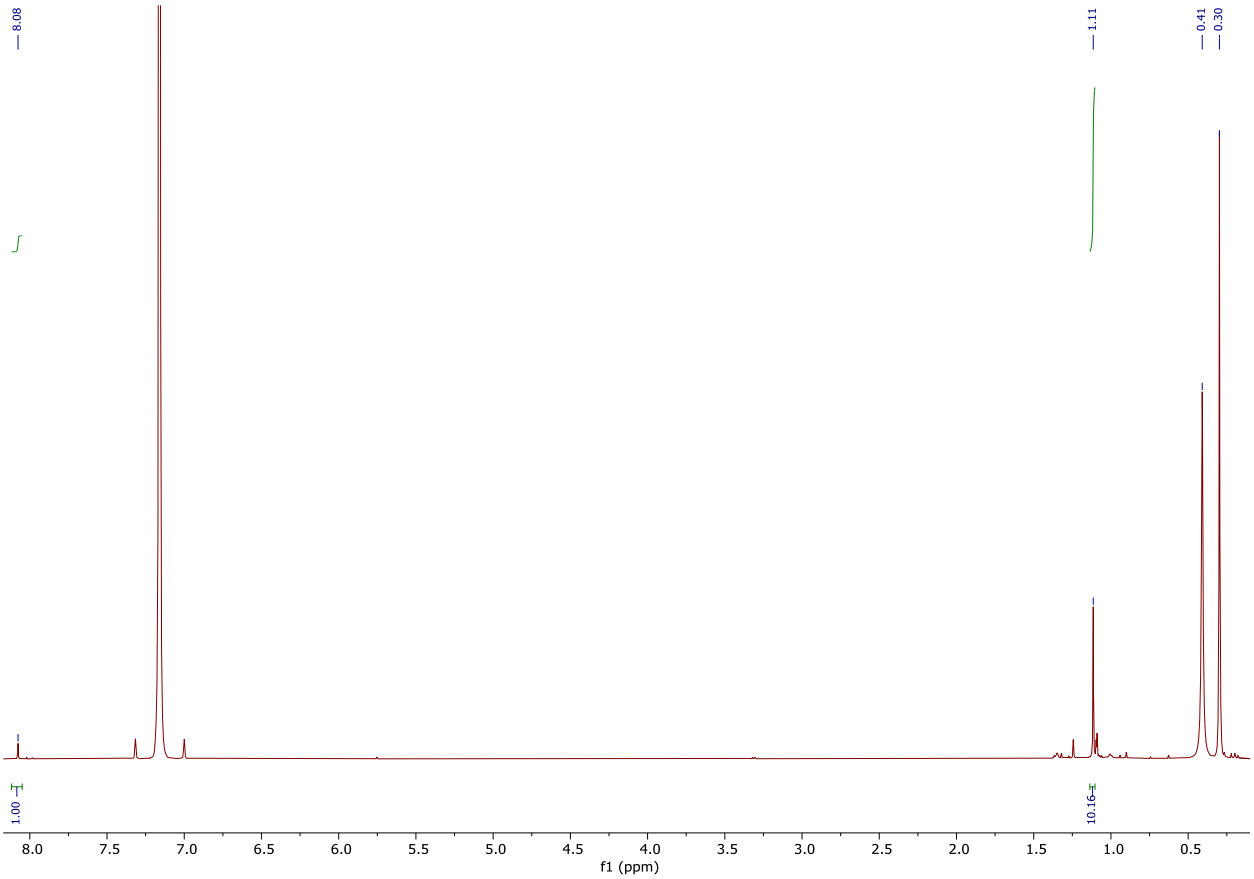

Figure S9. ^{1}H NMR spectrum in benzene-d_6 of the products formed after exposure of the ethyl-substituted compound **2** to air for 24 hours at 25 ºC.

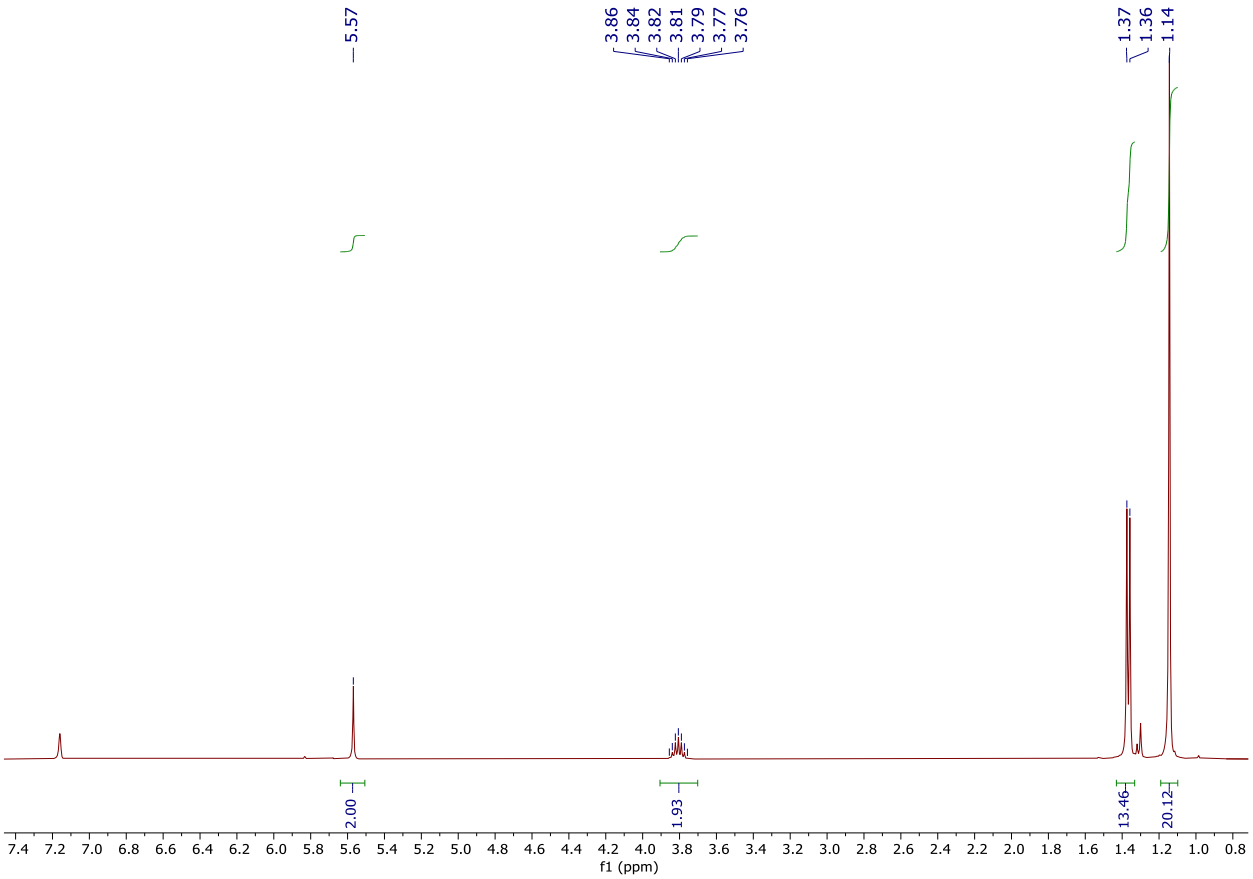

Figure S10. ^{1}H NMR spectrum of the *iso*-propyl substituted compound **3** at 25 ºC in benzene-d_6.

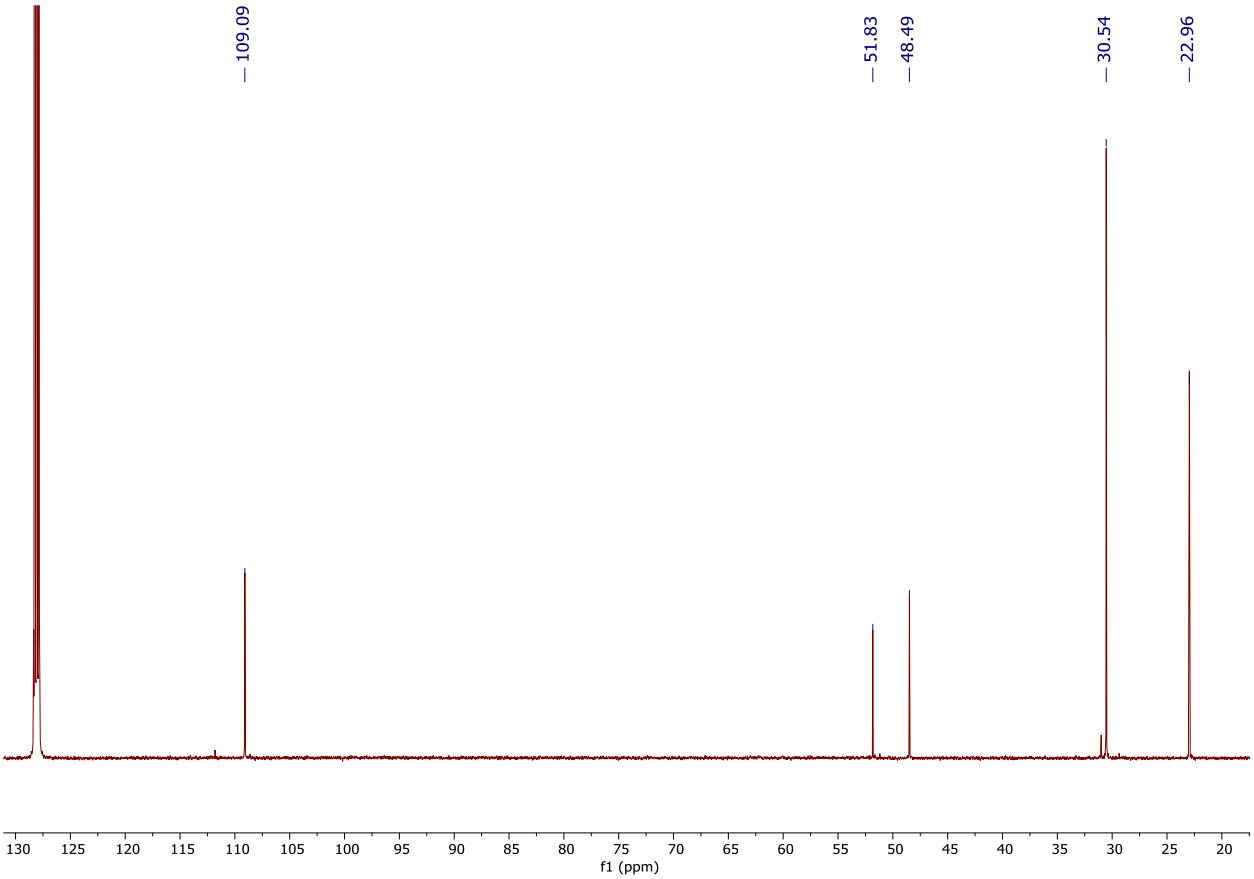

Figure S11. $^{13}C\{^{1}H\}$ NMR spectrum of the *iso*-propyl substituted compound **3** at 25 ºC in benzene-d_6.

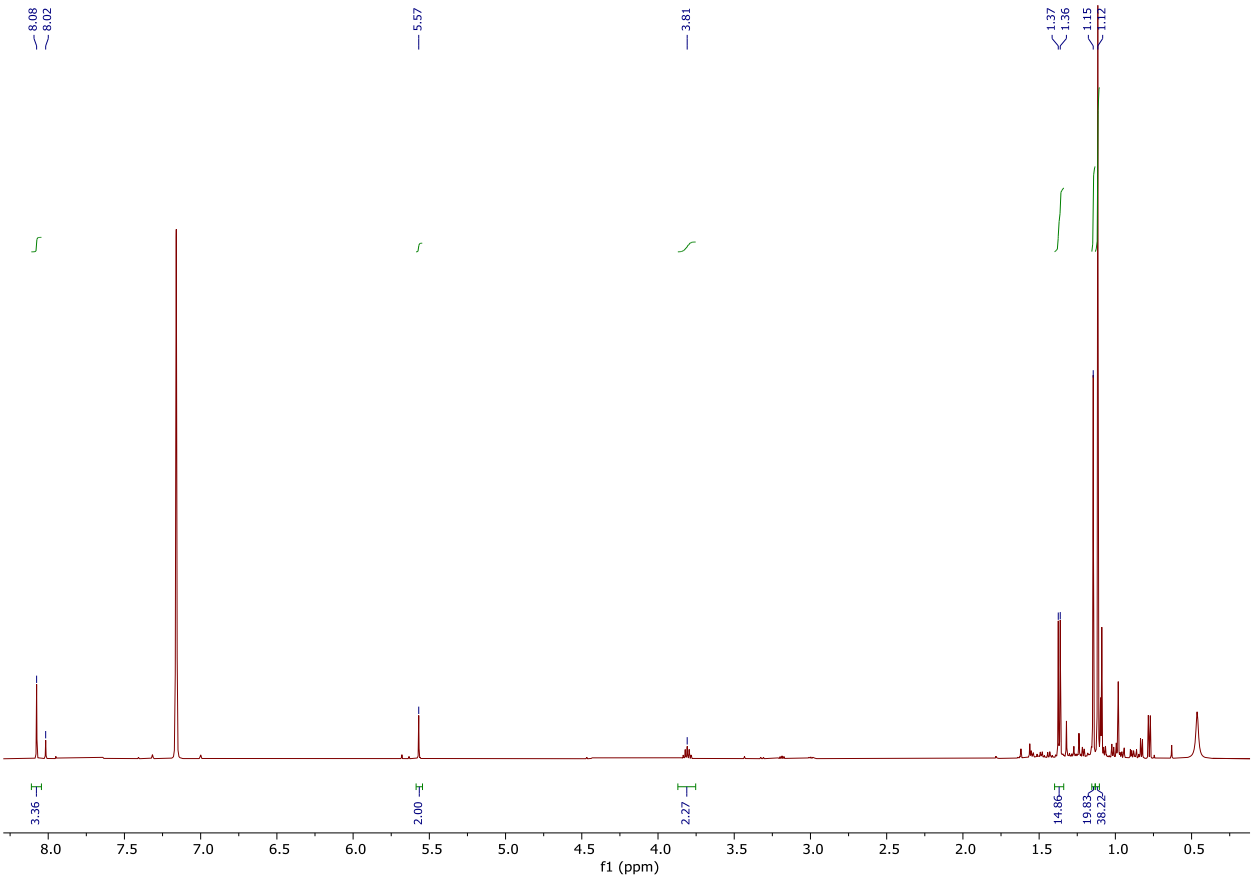

Figure S12. ^{1}H NMR spectrum in benzene-d_6 of the products formed after exposure of the *iso*-propyl substituted compound **3** to air for 24 hours at 25 ºC.

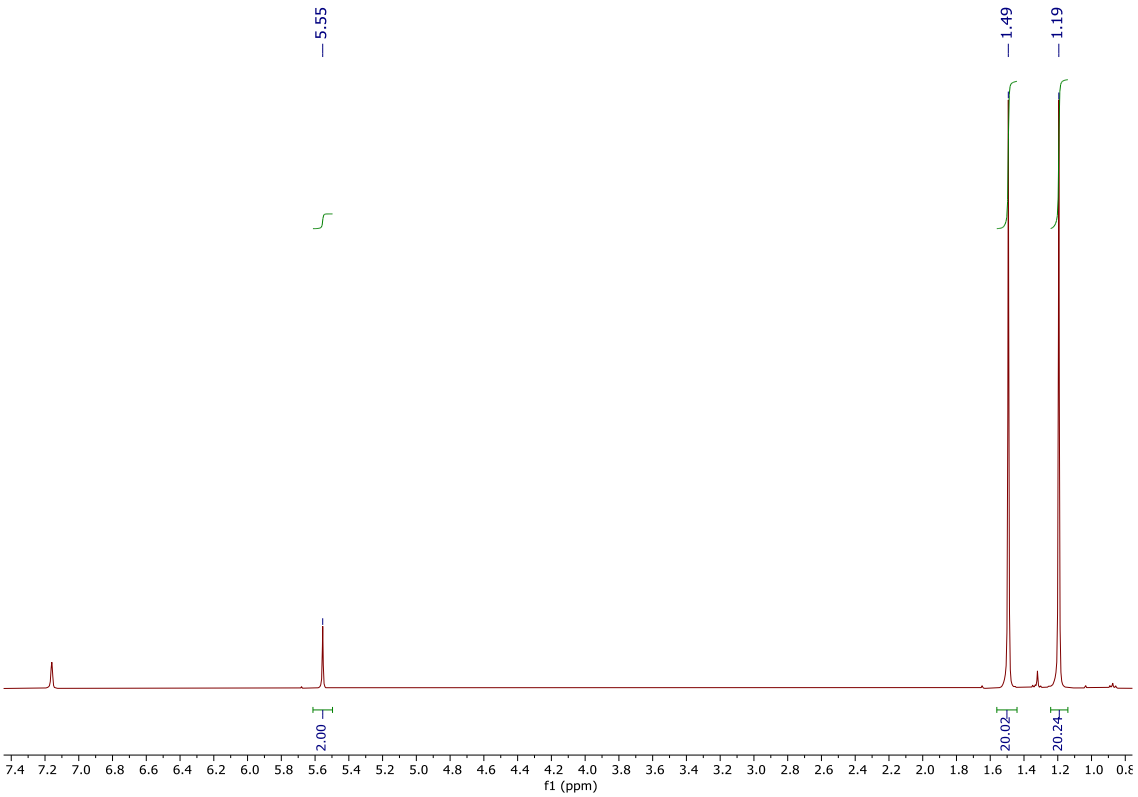

Figure S13. ^{1}H NMR spectrum of the *tert*-butyl substituted compound **4** at 25 ºC in benzene-d_6.

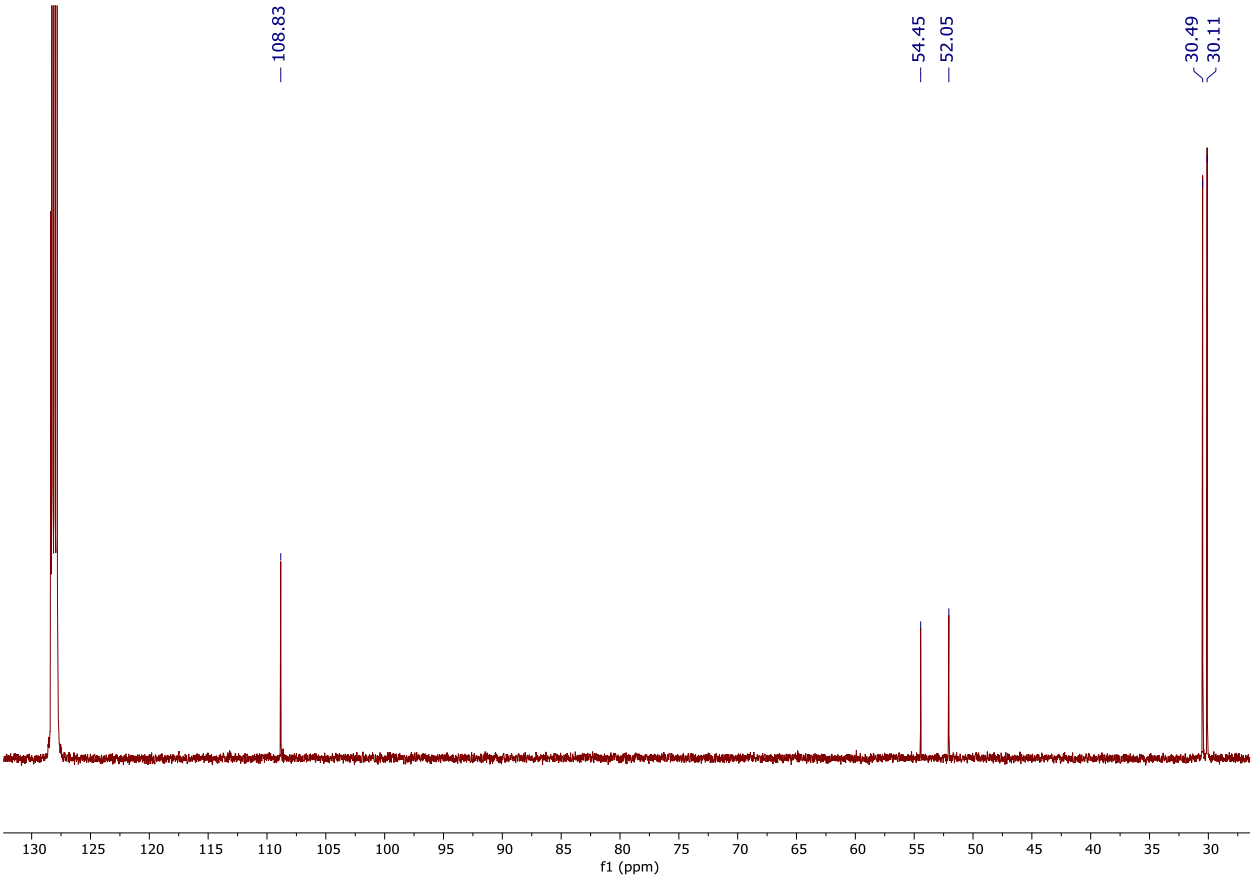

Figure S14. $^{13}C\{^{1}H\}$ NMR spectrum of the *tert*-butyl substituted compound **4** at 25 ºC in benzene-d_6.

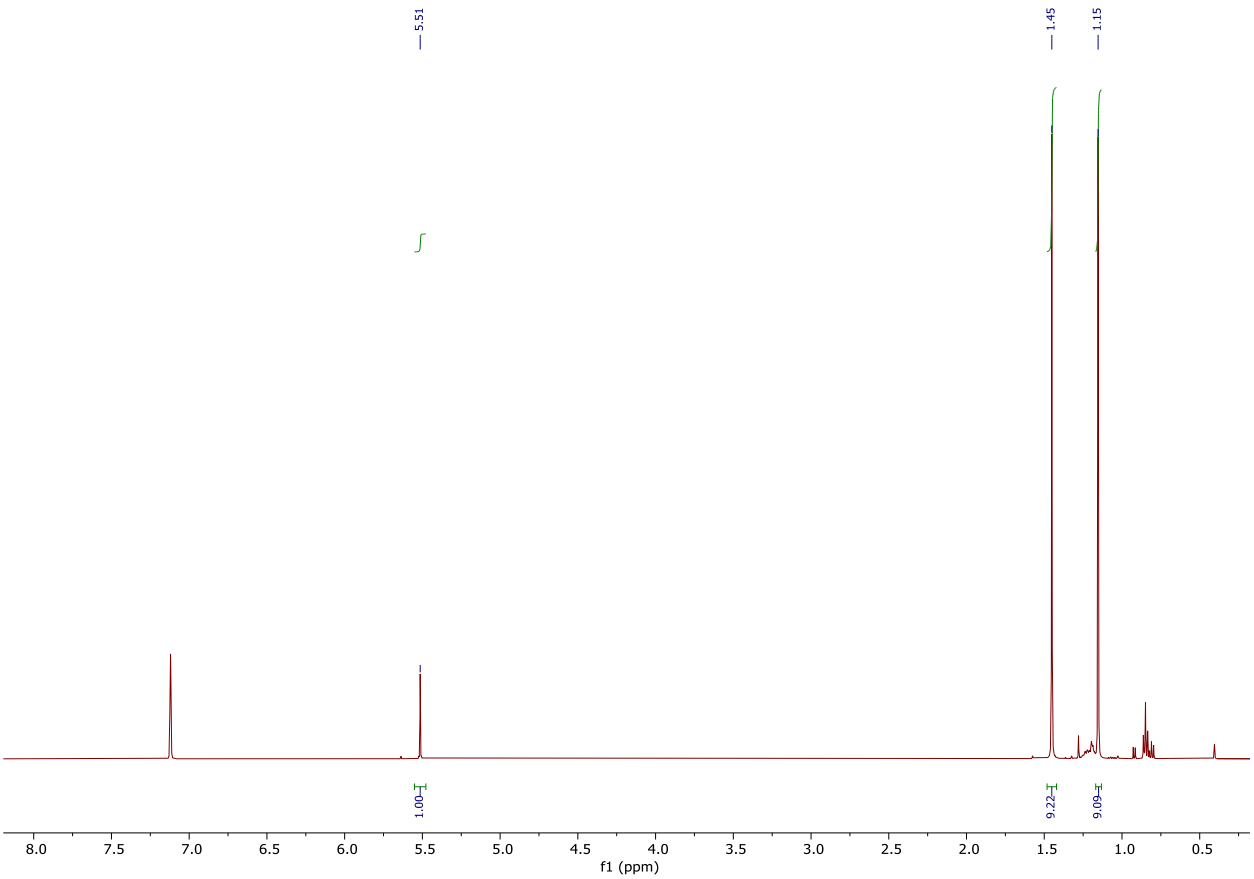

Figure S15. ^{1}H NMR spectrum in benzene-d_6 of the products after exposure of the *tert*-butyl substituted compound **4** to air for 72 hours at 25 ºC.

IR Spectra

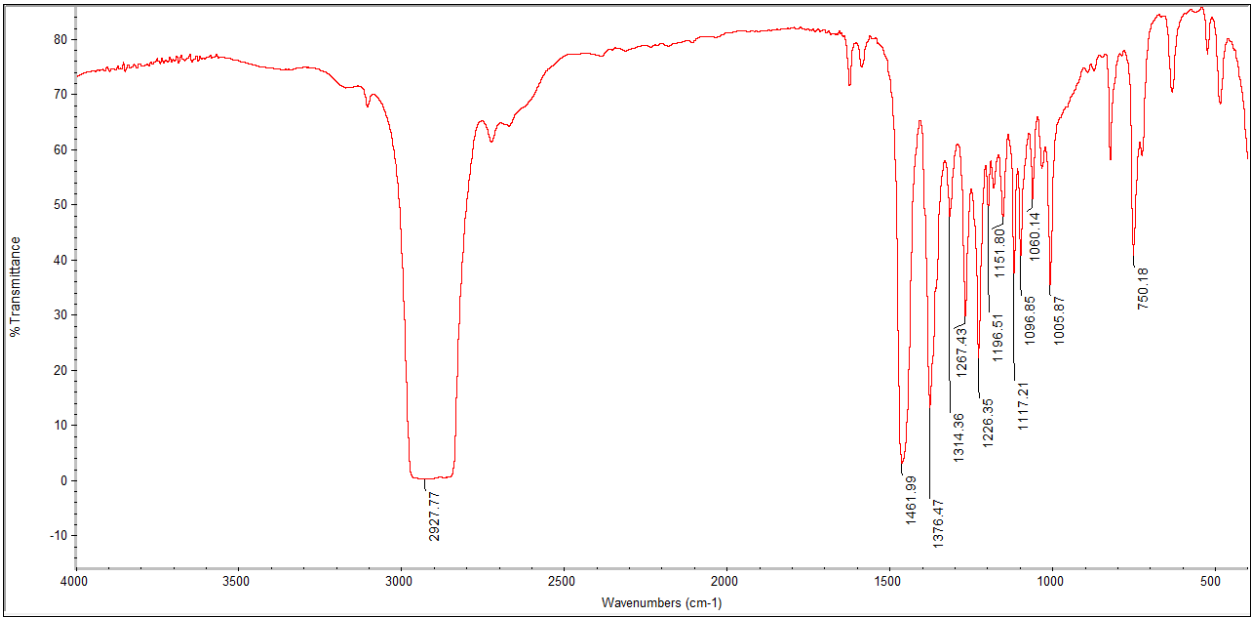

Figure S16. IR spectrum of the ethyl-substituted compound **2** collected as a Nujol mull between KBr plates.

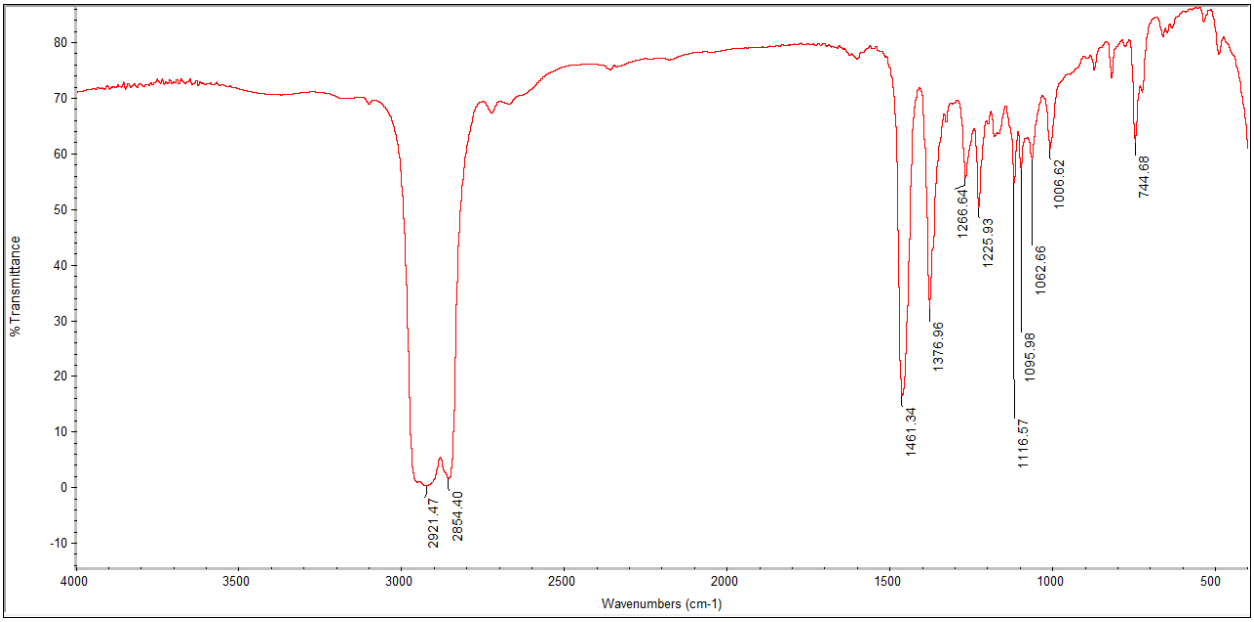

Figure S17. IR spectrum of the *iso*-propyl substituted compound **3** collected as a Nujol mull between KBr plates.

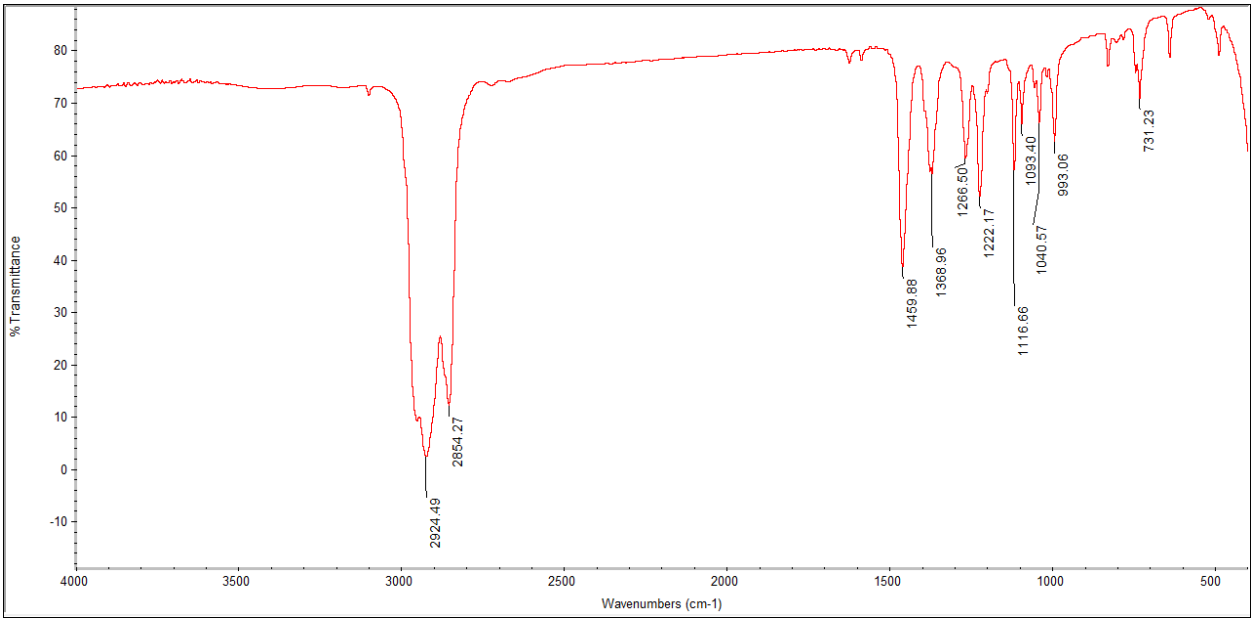

Figure S18. IR spectrum of the *tert*-butyl substituted compound **4** collected a Nujol mull between KBr plates.